Valence-band study of $Sm_{0.1}Ca_{0.9-x}Sr_xMnO_3$ using high-resolution ultraviolet photoelectron spectroscopy

M. K. Dalai,[1,2,*] B. R. Sekhar,[3] D. Biswas,[4] S. Thakur,[4] T.-C. Chiang,[1] D. Samal,[5,6] C. Martin,[7] and K. Maiti[4]

[1]*Department of Physics, University of Illinois at Urbana Champaign, 1110 West Green Street, Urbana, Illinois 61801, USA*

[2]*CSIR-National Physical Laboratory, Dr. K. S. Krishnan Marg, New Delhi-110012, India*

[3]*Institute of Physics, Sachivalaya Marg, Bhubaneswar-751005, India*

[4]*Department of Condensed Matter Physics and Materials' Science, Tata Institute of Fundamental Research, Colaba, Mumbai 400 005, India*

[5]*MESA+ Institute for Nanotechnology, University of Twente, Post Office Box 217, 7500AE Enschede, The Netherlands*

[6]*Max Planck Institute for Solid State Research, Heisenbergstraße 1, Stuttgart, Germany*

[7]*Laboratoire CRISMAT, UMR 6508 CNRS ENSICAEN, 6 Boulevard du Marechal Juin, 14050 Caen Cedex, France*

(Received 25 February 2014; revised manuscript received 5 June 2014; published 24 June 2014)

We have studied the concentration-dependent near-Fermi-level valence-band electronic structure of $Sm_{0.1}Ca_{0.9-x}Sr_xMnO_3$ ($x = 0$, 0.1, 0.3, and 0.6) using high-resolution ultraviolet photoelectron spectroscopy (HRUPS) across the metal insulator transition. At low temperatures (50 and 100 K), a transformation from pseudogap type behavior ($x = 0$ and 0.1) to insulating behavior ($x = 0.3$ and 0.6) is observed with an increase in Sr content. While at the high temperatures, the metalliclike density of states appears up to $x = 0.3$ and then vanishes at $x = 0.6$. The temperature-dependent spectra reveal a changeover from pseudogap to metalliclike states for $x = 0$ above its magnetic cluster-glass ordering temperature (110 K). In the case of $x = 0.1$, the temperature-dependent change in the density of states is quite different from that of $x = 0$ due to the weaker cluster-glass component and exhibits an interesting spectral weight transfer in the high-temperature paramagnetic phase. These findings would immensely help in understanding the puzzling charge transport scenario in $Sm_{0.1}Ca_{0.9-x}Sr_xMnO_3$ from a microscopic point of view.

DOI: 10.1103/PhysRevB.89.245131 PACS number(s): 71.20.−b, 71.30.+h, 75.47.Gk, 79.60.−i

I. INTRODUCTION

The tuning of the physical properties of manganites ($R_{1-x}A_xMnO_3$, where R and A are trivalent-rare earth and divalent-alkaline earth ions, respectively) is basically governed either chemically by changing the concentration and nature of the R and A cations [1,2] or physically by applying external stimuli viz. pressure [3–7], magnetic field [8–10], electric field [11–13], etc. Both physical and chemical parameters can dramatically influence the internal structure such as $Mn^{3+}(d^4)$/$Mn^{4+}(d^3)$ ratio, lattice distortion, and spin state. The electronic occupation at the Mn site and the lattice distortion controls, respectively the band filling and e_g bandwidth, thereby greatly influence the electronic properties of manganites. Vast majority of the scientific literature available so far is based on hole doped manganites because of their alluring colossal magnetoresistive effect [2]. Relatively less attention is paid to the electron doped system, which possesses somewhat similar as well as significantly different properties from its hole doped counterparts. Concerning the study on $R_{1-x}Ca_xMnO_3$, it is known that the paramagnetic (PM) state on the electron doped side exhibits metallic behavior even with a small injection of carriers ($x \geqslant 0.95$), in contrast to the hole doped side that exhibits insulating behavior [14–16]. In particular, the study on electron doped $Sm_{0.1}Ca_{0.9-x}Sr_xMnO_3$ has attracted great attention because of its unique structural, magnetic, and charge transport properties [16–19]. The observation of high-temperature thermoelectric response in electron-doped $CaMnO_3$ by Wang *et al.* [20] has added more momentum from an applied science point of view. $Sm_{0.1}Ca_{0.9}MnO_3$ corresponds to a ferromagneticlike metallic cluster-glass phase (with Curie temperature $T_C \sim 110$ K) embedded in a G-type antiferromagnetic (AFM) matrix. With the substitution of Sr for Ca ($x = 0.1$), the metallic state gets suppressed exhibiting an insulating behavior towards the low-temperature side (below ∼110 K). With the gradual increase in Sr concentration ($x = 0.1$–0.6), the insulating behavior becomes more pronounced and extends over a wide temperature range. From a magnetic point of view, the ferromagnetic (FM) component diminishes progressively with the increase in x and almost vanishes for $x \sim 0.2$. Surprisingly, an evolution of C-type antiferromagnetism sets in for the composition range, $0.2 \leqslant x \leqslant 0.6$, with the Neel temperature (T_N) ranging from 100 K to 240 K, and coexists along with the G-type phase in the low-temperature regime. In addition to sharply varying transport and magnetic phenomena in $Sm_{0.1}Ca_{0.9-x}Sr_xMnO_3$ with Sr doping, the structural study based on neutron diffraction by Martin *et al.* [17] also demonstrates a clear change in the crystal symmetry from $Pnma$ to $I4/mcm$ with the increase in Sr content.

Despite all such intriguing electronic/structural phenomena associated with $Sm_{0.1}Ca_{0.9-x}Sr_xMnO_3$, hardly anything is yet explored about the near Fermi energy, E_F electronic structure of this system. Since the charge transport and metallic magnetism is influenced greatly by the electronic states available close to E_F, it would be ideal to investigate how the near E_F electronic structure evolves when the system goes from a metallic to insulating state with an increase in Sr concentration. The detailed accurate knowledge about the near E_F electronic structure will elucidate our understanding in relation to the different competing electronic/magnetic phases manifested by $Sm_{0.1}Ca_{0.9-x}Sr_xMnO_3$. Keeping abreast of all the information, we have undertaken a high-resolution photoemission study of $Sm_{0.1}Ca_{0.9-x}Sr_xMnO_3$ ($x = 0$, 0.1,

*dalaimk@illinois.edu, dalaimk@nplindia.org

0.3, and 0.6) at various temperatures focusing on the few meV range in the vicinity of E_F to capture the underlying physics and shed light for further investigations. The high-energy resolution in this photoemission study enabled us to reveal interesting subtle features and their evolution with composition and temperature as discussed below.

II. EXPERIMENT

The polycrystalline samples of $Sm_{0.1}Ca_{0.9-x}Sr_xMnO_3$, $x =$ 0, 0.1, 0.3, and 0.6 were prepared using the high temperature solid state reactions method. The details of the sample preparation technique were published elsewhere [17]. Purity of the samples was confirmed by x-ray powder diffraction patterns exhibiting highly pure samples in single phase. The studies of the structural, transport, and magnetic properties of these samples were published earlier [17]. The high-resolution ultraviolet photoelectron spectroscopy measurements were performed using a monochromatic He I (21.2 eV) photon source. The photoelectrons were collected using a Gammadata Scienta R4000WAL electron energy analyzer equipped with an ultrahigh vacuum experimental chamber. Since the spectral intensity at the Fermi level is week in these materials, the energy resolution was set at 5 meV instead of 1.5 meV to have improved signal to noise ratio that enabled studying the finer changes near the Fermi level. The sample surfaces were cleaned using scrapers (fine grained diamond files) under a base vacuum better than $\sim 1.0 \times 10^{-10}$ mbar before taking the data at each temperature. Separate scrapers were used to clean each sample, and reproducibility of the data was verified after each cleaning cycle. The low-temperature measurements were carried out using an open cycle helium cryostat by pumping liquid helium through the sample manipulator.

III. RESULTS AND DISCUSSION

The Sr concentration-dependent valence-band spectra of $Sm_{0.1}Ca_{0.9x}Sr_xMnO_3$ ($x = 0$, 0.1, 0.3, and 0.6) at 50 K is presented in Fig. 1. The observed features in the spectra (Fig. 1) are the characteristics of manganites studied earlier [21–28]. However, our present focus here is to investigate the finer variations of the electronic states in the vicinity of the Fermi level. The valence-band spectra of manganites are mainly dominated by the Mn $3d$ and O $2p$ states. The spectroscopic signatures corresponding to these states are clearly observed in the figure. The broad feature appearing at around 5.8 eV (marked D) is due to the Mn-O bonding states. The features in the energy range 1.5–4 eV binding energies are attributed to Mn $3d$ t_{2g} (marked B) and nonbonding O $2p$ (marked C) contributions. The most important feature is a tail-like structure near the Fermi level, E_F (marked A) corresponding to the Mn $3d$ e_g states. The high-resolution spectra corresponding to the near E_F e_g states will be shown in the subsequent section, where the spectra have been normalized to the integrated intensity in the binding energy range around 0.25 eV.

The electronic states near the Fermi level are mostly responsible for governing the electronic properties of these materials. From our high-resolution photoemission study, we observed various unique changes associated with the near E_F states as a function of Sr concentration as well as temperature for $Sm_{0.1}Ca_{0.9-x}Sr_xMnO_3$. The x-dependent near-E_F states

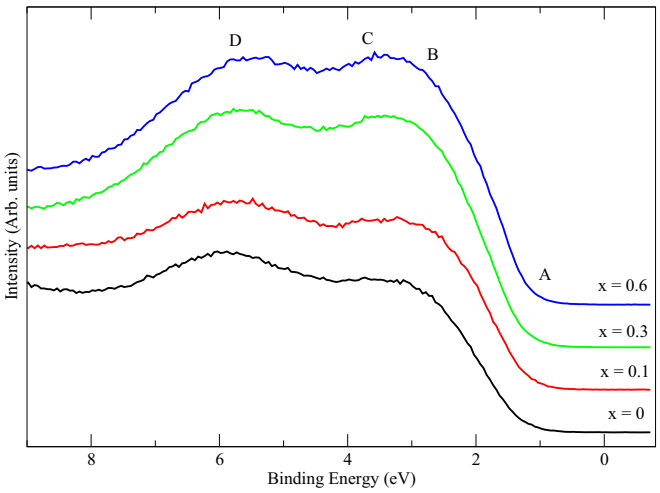

FIG. 1. (Color online) The valence-band spectra of $Sm_{0.1}Ca_{0.9-x}Sr_xMnO_3$ at 50 K for various concentrations $x =$ 0, 0.1, 0.3 and 0.6 are produced using high-resolution ultraviolet photoelectron spectroscopy (HRUPS) having photon energy 21.2 eV (He I). The mark **A** corresponds to the e_g states of the MnO_6 octahedra, the mark **B** corresponds to the t_{2g} states, mark **C** corresponds to the nonbonding O $2p$ states and the mark **D** corresponds to the bonding states of the MnO_6 octahedra.

for $Sm_{0.1}Ca_{0.9x}Sr_xMnO_3$ at 50 K are presented in Fig. 2(a). For the $x = 0$ sample, the density of states is finite at E_F. With the increase of x, the density of states gradually decreases and reaches a minimum for $x = 0.3$ and 0.6, with almost no finite states at the Fermi level. Moreover, no distinct spectral change is observed between $x = 0.3$ and 0.6 at 50 K. At $T = 100$ K, the spectral change as a function of x [Fig. 2(b)] exhibits almost similar behavior as compared to that at 50 K, except a little difference between $x = 0$ and 0.1, which corresponds to a relatively smaller change than the former case. Most interestingly, the concentration-dependent high-temperature (200 and 295 K) spectra [Figs. 2(c) and 2(d)] are found to be different than that of the low-temperature ones. At both 200 and 295 K, the finite number of states are observed at the

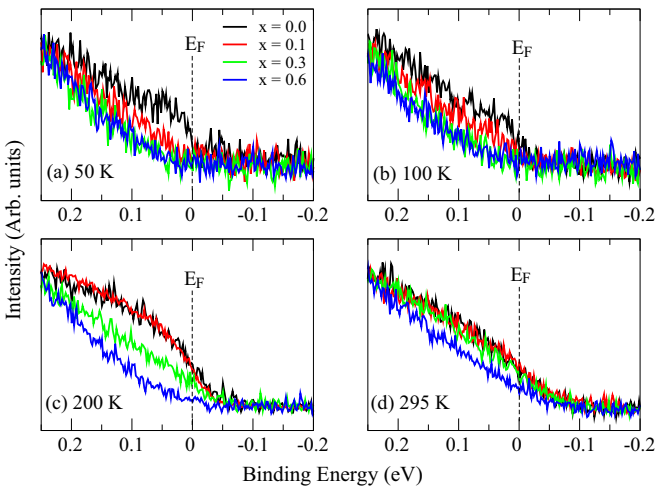

FIG. 2. (Color online) The high resolution near E_F e_g states of $Sm_{0.1}Ca_{0.9-x}Sr_xMnO_3$ (x = 0, 0.1, 0.3 and 0.6) at 50 K (a), 100 K (b), 200 K (c) and 295 K (d).

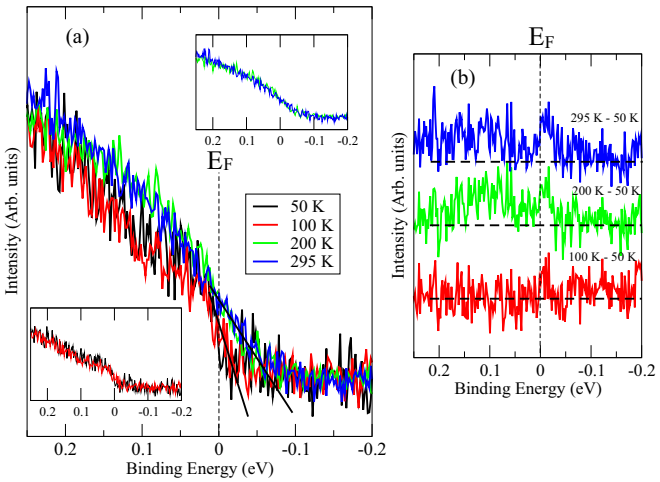

FIG. 3. (Color online) (a) The high resolution near E_F e_g states of $Sm_{0.1}Ca_{0.9}MnO_3$ at 50, 100, 200, and 295 K respectively. The buttom inset shows the comparison of 50 and 100 K spectra and the top inset shows the comparison of 200 and 295 K spectra. The solid lines marked on the spectra distinguish the band edge at different temperatures. (b) The difference of 50 K spectra from that of 100, 200, and 295 K.

Fermi level for $x = 0, 0.1$, and 0.3, whereas the corresponding states vanish for $x = 0.6$. Moreover, a careful inspection of the high-temperature spectra reveals a relatively less electronic occupation near the E_F for $x = 0.3$ as compared to that of $x = 0$ and 0.1. However, no noticeable change in the electronic occupation is observed between the spectra for $x = 0$ and $x = 0.1$ at 200 and 295 K, respectively.

In Figs. 3 and 4, we present the temperature evolution of near-E_F spectra for two cluster glass phases ($x = 0$ and 0.1) down to 50 K. For $x = 0$ [Fig. 3(a)], no appreciable

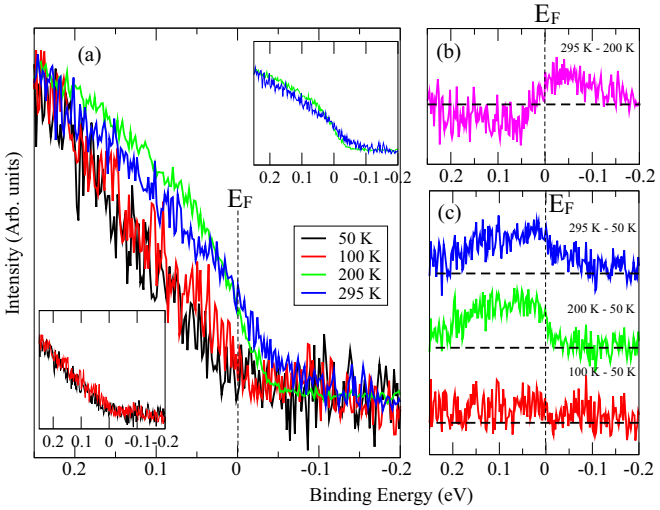

FIG. 4. (Color online) The high resolution near E_F e_g states of $Sm_{0.1}Ca_{0.8}Sr_{0.1}MnO_3$ at 50, 100, 200, and 295 K respectively. The bottom inset shows the comparison of 50 and 100 K spectra and the top inset shows the comparison of 200 and 295 K spectra. (b) The difference spectra (295 K–200 K) represent the spectral weight transfer at the Fermi level. (c) The difference of 50 K spectra from that of 100, 200, and 295 K.

change in the spectral shape is observed, when we increase the temperature from 50 to 100 K. The inset (bottom) in Fig. 3 shows a clear comparison of these two spectra. With the increase in temperature to 200 K, the spectral shape changes with a slight increase in intensity and a broadening of the e_g band across the Fermi level, which is marked by putting a line at the band edge. With further increase in temperature to 295 K, we hardly observe any difference in the spectral shape as compared to that of 200 K. The inset (top) in Fig. 3 shows the clear comparison of these two spectra. The spectral variation with the temperature is also presented in Fig. 3(b) as the difference spectra. For $x = 0.1$ (Fig. 4), substantial changes in the spectra are observed, when we move from the lower temperature regime (50 and 100 K) to the higher temperature regime (200 and 294 K). With the increase of temperature from 50 to 100 K, a small increase of intensity around 30 meV below the Fermi level is observed. A clear comparison of these two spectra is shown as the inset (bottom) of Fig. 4. With further increase of temperature from 100 to 200 K, the intensity of the spectral weight increases. The magnitude of the changes is quite large in comparison to that of $x = 0$. The most interesting temperature-dependent spectral change for $x = 0.1$ is observed by further increasing the temperature to 295 K, which is shown as the top inset in Fig. 4. A clear spectral weight transfer is observed at 295 K, where some of the electronic states are transferred towards the conduction band (at/above the Fermi level) resulting in the broadening of valence-band spectra. The difference between 200 and 295 K spectra in Fig. 4(b) is also a clear representation of the spectral weight transfer. It is also found that the two spectra (200 and 295 K) cross each other around 15 meV below the Fermi level. The overall variations of the spectra from the lowest temperature are presented in Fig. 4(c) as the difference spectra.

To start with the discussion on concentration-dependent changes in the near E_F electronic states of $Sm_{0.1}Ca_{0.9-x}Sr_xMnO_3$, we have already brought out a few points as mentioned in the introduction. Below 110 K, the parent compound $Sm_{0.1}Ca_{0.9}MnO_3$ exhibits a FM-like metallic-cluster glass phase embedded in a G-type AFM insulating matrix. The metallic conduction in such phase-separated systems can be attributed to the small number of electrons (mobile) in the e_g state [24,28,29]. However, the majority of the electrons are localized forming the G-type AFM insulating phase. Based on this hypothesis, there will be a finite but suppressed density of states near the Fermi level, and it will be quite different from what is generally observed for the conventional metallic phases. The spectra in Figs. 2(a) and 2(b) clearly indicate the signature of suppressed density of states for $Sm_{0.1}Ca_{0.9}MnO_3$. With Sr doping, the FM metallic state gets suppressed, and its signature is evident by recognizing the decreased density of states in the e_g band [Figs. 2(a) and 2(b)]. Here the density of e_g states for $x = 0.3$ and 0.6 samples almost disappears with the formation of an insulating gap at the Fermi level. Based on earlier reports [22,23,27,28,30–34] the suppressed density of states at the Fermi level could be due to the disorder/mixed phase (FM metallic and AFM insulating) and is generally described in terms of a pseudogap phase. The pseudogaplike behavior in the $Sm_{0.1}Ca_{0.9-x}Sr_xMnO_3$ system is found to gradually evolve into normal insulating behavior [Figs. 2(a) and 2(b)] with the increase in Sr concentration.

The Sr concentration-dependent electronic structure of $Sm_{0.1}Ca_{0.9-x}Sr_xMnO_3$ at various temperatures is found to be quite interesting. As per earlier reports [16,17,19], the samples corresponding to $x = 0$, 0.1, and 0.3 exhibit PM metallic behavior at room temperature, whereas the sample with $x = 0.6$ exhibits insulating behavior. In Fig. 2(d), a clear signature of the high density of e_g states along with the broadening of the valence band has been observed for $x = 0$, 0.1, and 0.3 in contrast with the case for $x = 0.6$. While at 200 K, the samples with $x = 0$ and 0.1 retain metallic behavior as observed at room temperature, whereas the sample with $x = 0.3$ exhibits a decreased metallicity and then insulating behavior in the case for $x = 0.6$. This is clearly demonstrated in Fig. 2(c) that shows a high density of e_g states for $x = 0$ and 0.1 and then decreases for $x = 0.3$ and shows sharply diminished e_g states for $x = 0.6$. The reduced metallic carriers in $Sm_{0.1}Ca_{0.9-x}Sr_xMnO_3$ with Sr substitution are linked to its structural modification. From the x-ray and neutron diffraction studies [17], it has been observed that, at room temperature, the system undergoes a structural change from $Pnma$ to $I4/mcm$ with the substitution of Sr, where the MnO_6 octahedra get distorted and elongated along the c axis, leading to weaker Mn $3d$-O $2p$ hybridization. This can directly influence the internal band structure resulting in charge localization and thereby reduced carrier mobility.

To have further insight into the pseudogap behavior of $Sm_{0.1}Ca_{0.9}MnO_3$, we discuss here the distinct results inferred from the low- (50 and 100 K) and high- (200 and 295 K) temperature spectra (Fig. 3). Clearly, we observe a suppressed density of states at low temperatures (50 and 100 K) in contrast to the relatively higher density of states at 200 and 295 K. This suggests that the low-temperature pseudogaplike phase gradually transforms to a fully metalliclike phase with the increase of temperature. With the introduction of Sr at the Ca site ($x = 0.1$), the cluster-glass-like metallic state gets suppressed in the low-temperature regime, however, the high-temperature phase remains as metallic as that of $x = 0$. The spectra in Fig. 4 clearly indicate a transformation to the metallic behavior at higher temperatures. This phenomena could have its origin linked to the thermally activated mobile electrons in the e_g states as reported earlier for other manganites [35–37]. Notably, we observe a spectral weight transfer along with the e_g band broadening, when temperature rises from 200 to 295 K (top inset in Fig. 4). This is reminiscent of a phase transition scenario where the system changes to a different state as a function of temperature. However, in our case this is observed in the same high-temperature paramagnetic metallic state. Had it been only due to the thermal activation process, we should expect to observe similar effects in other compositions as well. We conjecture that there must be some kind of inherent electronic reconstruction taking place in response to the change of temperature in the paramagnetic state for $x = 0.1$, which gives rise to such an effect. It could be a crossover from bad to good metallic behavior. The detailed understanding of this anomalous behavior invites further studies including theoretical calculations as well. It is to be noted here that a very recent study on nickelates based on optical conductivity by R. Jarmillo *et al.* [38] also observed a similar kind of spectral weight redistribution in the paramagnetic phase, highlighting the importance of this effect. In essence, our findings based on photoemission study highlight unusual phenomena, where the high-temperature paramagnetic state is found to be more metallic than the low-temperature phase. This is unlike the case of well studied double exchange favorable metallic manganites [24,39–41], where a higher electronic density of states near the E_F is observed at low temperatures.

IV. CONCLUSIONS

We presented a comprehensive investigation of the near E_F valence-band electronic structure of $Sm_{0.1}Ca_{0.9-x}Sr_xMnO_3$ ($x = 0$, 0.1, 0.3, and 0.6) using high-resolution ultraviolet photoelectron spectroscopy at various temperatures. Albeit the substitution of iso-valent Sr at Ca sites that adds neither electrons nor holes to the system, we find dramatic changes in the near E_F electronic states. At low temperatures (50 and 100 K), we observed a finite density of states exhibiting pseudogap behavior for the cluster glass compositions ($x = 0$ and 0.1). The low-temperature electronic density of states gradually decreases with the increase of Sr concentration, and therefore the pseudogap in the parent compound $Sm_{0.1}Ca_{0.9}MnO_3$ turns into an insulating gap for $x = 0.3$ and 0.6. Moreover, noticeable spectral changes were observed at higher temperatures (200 and 295 K), where a metalliclike high density of e_g states with band broadening was observed for $x = 0$, 0.1, and 0.3 in sharp contrast to $x = 0.6$. We have also studied the temperature-dependent near-E_F valence band of $Sm_{0.1}Ca_{0.9}MnO_3$ and $Sm_{0.1}Ca_{0.8}Sr_{0.1}MnO_3$ and observed a transformation from low-temperature pseudogaplike states to metalliclike states with the increase in temperature. Besides, a spectral weight transfer towards the Fermi level was also observed for $Sm_{0.1}Ca_{0.8}Sr_{0.1}MnO_3$ (by changing the temperature from 200 to 295 K) that signifies a possible crossover from bad to good metallic behavior in the high-temperature paramagnetic phase. We discussed all the above mentioned results by considering the electronic and/or magnetic phase separation as well as the structural transition associated with the $Sm_{0.1}Ca_{0.9-x}Sr_xMnO_3$ system.

ACKNOWLEDGMENTS

M.K.D. acknowledges the Indo-US Science and Technology Forum (IUSSTF) for granting the fellowship to work at University of Illinois at Urbana Champaign, USA. T.C.C. acknowledges the financial support of the US Department of Energy, Office of Science, under Grant No. DE-FG02-07ER46383. K.M. acknowledges financial support of the Department of Science and Technology under the Swarnajayanti Fellowship program.

[1] M. B. Salamon and M. Jaime, Rev. Mod. Phys. **73**, 583 (2001).
[2] A. P. Ramirez, J. Phys. Condens. Matter. **9**, 8171 (1997).
[3] Y. Moritomo, H. Kuwahara, Y. Tomioka, and Y. Tokura, Phys. Rev. B **55**, 7549 (1997).

[4] C. Meneghini, D. Levy, S. Mobilio, M. Ortolani, M. Nunez-Reguero, Ashwani Kumar, and D. D. Sarma, Phys. Rev. B **65**, 012111 (2001).

[5] A. Congeduti, P. Postorino, P. Dore, A. Nucara, S. Lupi, S. Mercone, P. Calvani, A. Kumar, and D. D. Sarma, Phys. Rev. B **63**, 184410 (2001).

[6] P. Postorino, A. Congeduti, P. Dore, A. Sacchetti, F. Gorelli, L. Ulivi, A. Kumar, and D. D. Sarma, Phys. Rev. Lett. **91**, 175501 (2003).

[7] Yang Ding, Daniel Haskel, Yuan-Chieh Tseng, Eiji Kaneshita, Michel van Veenendaal, J. F. Mitchell, Stanislav V. Sinogeikin, Vitali Prakapenka, and Ho-kwang Mao, Phys. Rev. Lett. **102**, 237201 (2009).

[8] H. Kuwahara, Y. Tomioka, A. Asamitsu, Y. Moritomo, and Y. Tokura, Science **270**, 961 (1995).

[9] Y. Tomioka, A. Asamitsu, H. Kuwahara, Y. Moritomo, and Y. Tokura, Phys. Rev. B **53**, R1689 (1996).

[10] Y. Tomioka, A. Asamitsu, Y. Moritomo, H. Kuwahara, and Y. Tokura, Phys. Rev. Lett. **74**, 5108 (1995).

[11] K. Miyano, T. Tanaka, Y. Tomioka, and Y. Tokura, Phys. Rev. Lett. **78**, 4257 (1997).

[12] A. Odagawa, H. Sato, I. H. Inoue, H. Akoh, M. Kawasaki, Y. Tokura, T. Kanno, and H. Adachi, Phys. Rev. B **70**, 224403 (2004).

[13] S. Dong, C. Zhu, Y. Wang, F. Yuan, K. F. Wang, and J-M. Liu, J. Phys. Condens. Matter. **19**, 266202 (1997).

[14] C. Martin, A. Maignan, M. Hervieu, and B. Raveau, Phys. Rev. B **60**, 12191 (1999).

[15] A. Maignan, C. Martin, F. Damay, and B. Raveau, Chem. Mater **10**, 950 (1998).

[16] J. Hejtmanek, Z. Jirak, M. Marysko, C. Martin, A. Maignan, M. Hervieu, and B. Raveau, Phys. Rev. B **60**, 14057 (1999).

[17] C. Martin, A. Maignan, M. Hervieu, S. Hébert, A. Kurbakov, G. André, F. Bourée-Vigneron, J. M. Broto, H. Rakoto, and B. Raquet, Phys. Rev. B **77**, 054402 (2008), and references therein.

[18] M. Respaud, J. M. Broto, H. Rakoto, J. Vanacken, P. Wagner, C. Martin, A. Maignan, and B. Raveau, Phys. Rev. B **63**, 144426 (2001).

[19] C. Martin, A. Maignan, M. Hervieu, B. Raveau, Z. Jirak, M. M. Savosta, A. Kurbakov, V. Trounov, G. Andre, and F. Bouree, Phys. Rev. B **62**, 6442 (2000).

[20] Yang Wang, Yu Sui, Hongjin Fan, Xianjie Wang, Yantao Su, and Xiaoyang Liu, Chem. Mater. **21**, 4653 (2009).

[21] T. Saitoh, A. E. Bocquet, T. Mizokawa, H. Namatame, A. Fujimori, M. Abbate, Y. Takeda, and M. Takano, Phys. Rev. B **51**, 13942 (1995).

[22] K. Ebata, H. Wadati, M. Takizawa, A. Fujimori, A. Chikamatsu, H. Kumigashira, M. Oshima, Y. Tomioka, and Y. Tokura, Phys. Rev. B **74**, 064419 (2006).

[23] K. Ebata, M. Hashimoto, K. Tanaka, A. Fujimori, Y. Tomioka, and Y. Tokura, Phys. Rev. B **76**, 174418 (2007).

[24] M. K. Dalai, P. Pal, B. R. Sekhar, N. L. Saini, R. K. Singhal, K. B. Garg, B. Doyle, S. Nannarone, C. Martin, and F. Studer, Phys. Rev. B **74**, 165119 (2006).

[25] M. K. Dalai, P. Pal, R. Kundu, B. R. Sekhar, S. Banik, A. K. Shukla, S. R. Barman, and C. Martin, Physica B **405**, 186 (2010).

[26] M. K. Dalai, P. Pal, B. R. Sekhar, M. Merz, P. Nagel, S. Schuppler, and C. Martin, Phys. Rev. B **85**, 155128 (2012).

[27] P. Pal, M. K. Dalai, R. Kundu, M. Chakraborty, B. R. Sekhar, and C. Martin, Phys. Rev. B **76**, 195120 (2007).

[28] P. Pal, M. K. Dalai, R. Kundu, B. R. Sekhar, and C. Martin, Phys. Rev. B **77**, 184405 (2008).

[29] R. Bindu, G. Adhikary, S. Pandey, S. K. Patil, and K. Maiti, New J. Phys. **12**, 033026 (2010).

[30] R. Bindu, Ganesh Adhikary, Nishaina Sahadev, N. P. Lalla, and Kalobaran Maiti, Phys. Rev. B **84**, 052407 (2011).

[31] D. D. Sarma, A. Chainani, S. R. Krishnakumar, E. Vescovo, C. Carbone, W. Eberhardt, O. Rader, Ch. Jung, Ch. Hellwig, W. Gudat, H. Srikanth, and A. K. Raychaudhuri, Phys. Rev. Lett. **80**, 4004 (1998).

[32] M. Kobayashi, K. Tanaka, A. Fujimori, Sugata Ray, and D. D. Sarma, Phys. Rev. Lett. **98**, 246401 (2007).

[33] K. Maiti, R. S. Singh, and V. R. R. Medicherla, Europhys. Lett. **78**, 17002 (2007).

[34] Deepnarayan Biswas, Nishaina Sahadev, Ganesh Adhikary, Geetha Balakrishnan, and Kalobaran Maiti, Phys. Rev. B **88**, 134405 (2013).

[35] W. Bao, J. D. Axe, C. H. Chen, and S. W. Cheong, Phys. Rev. Lett. **78**, 543 (1997).

[36] H. L. Liu, S. L. Cooper, and S-W. Cheong, Phys. Rev. Lett. **81**, 4684 (1998).

[37] H. M. Rønnow, Ch. Renner, G. Aeppli, T. Kimura, and Y. Tokura, Nature (London) **440**, 1025 (2006).

[38] R. Jaramillo, Sieu D. Ha, D. M. Silevitch, and Shriram Ramanathan, Nat. Phys. **10**, 304 (2014).

[39] J.-H. Park, C. T. Chen, S-W. Cheong, W. Bao, G. Meigs, V. Chakarian, and Y. U. Idzerda, Phys. Rev. Lett. **76**, 4215 (1996).

[40] D. D. Sarma, N. Shanthi, S. R. Krishnakumar, T. Saitoh, T. Mizokawa, A. Sekiyama, K. Kobayashi, A. Fujimori, E. Weschke, R. Meier, G. Kaindl, Y. Takeda, and M. Takano, Phys. Rev. B **53**, 6873 (1996).

[41] T. Saitoh, A. Sekiyama, K. Kobayashi, T. Mizokawa, A. Fujimori, D. D. Sarma, Y. Takeda, and M. Takano, Phys. Rev. B **56**, 8836 (1997).